

Assessing the Performance of Computational Methods for the Prediction of the Ground State Structure of a Cyclic Decapeptide

Manuel Doemer,^[a] Matteo Guglielmi,^[a] Prashanth Athri,^[a] Natalia S. Nagornova,^[b] Thomas R. Rizzo,^[b] Oleg V. Boyarkin,^[b] Ivano Tavernelli,^[a] and Ursula Rothlisberger^{[a]*}

We benchmark the performance of various computational approaches, ranging from the classical nonpolarizable force fields AMBER FF96 and FF99SB, the polarizable force fields AMBER FF02polEP and AMOEBAbio09 to the semiempirical DFT method SCC-DFTB. The test set consists of nine conformations of gas-phase protonated gramicidin S, a cyclic decapeptide. We discuss their structural features in relation to the intrinsic lowest energy structure, which has been solved recently by a combination of cold ion spectroscopy and high level theoretical methods (Nagornova et al., *Angew Chem Int Ed* 2011, 50, 5383). As a reference, we use the energetics at the M05-2X level of theory. The latter has been

validated as a suitable reference method in predicting the correct ground state structure of gas-phase protonated bare and micro-solvated tryptophan as well as gas-phase protonated gramicidin S by comparison to experiment. We discuss the performance of the different more approximate methods in relation to their potential use as efficient and reliable tools to explore conformational space for the generation of candidate structures before refinement at the DFT level. © 2012 Wiley Periodicals, Inc.

DOI: 10.1002/qua.24085

Introduction

The structure and function of bio-molecular systems are closely linked, and the determination of the native structure is often the basis for an understanding of the biological function and mechanism of action.

Various methods such as X-ray or neutron diffraction, NMR, IR, Raman or microwave spectroscopy are available to obtain structural information. All of these techniques have inherent advantages and disadvantages and differ in the type of information they provide as well as in the applied measuring conditions, that might deviate to varying degrees from the *in vivo* physiological conditions.

Except for diffraction methods, none of the aforementioned techniques is able to measure directly the molecular structure. Structures can only be calculated by theoretical methods, which in turn have to be validated by comparing predicted physical properties with experiment. In the case of IR spectroscopy, for instance, the compared quantity can be frequencies and intensities of vibrational transitions, which are directly linked to the molecular structure. Theoretical methods are therefore, in conjunction with experiment, inherent parts of any procedure that targets the determination of molecular structure. However, the small energy separations between different conformational states pose stringent requirements on the accuracy of the computational method, which necessitates the use of high-level approaches. In contrast, even comparably small-sized systems span a relatively large conformational space for which a comprehensive conformational search is only possible with computationally more expedient methods. Density functional methods usually represent a good trade-off between computational cost and accuracy. Especially modern exchange correlation

functionals with an improved functional form of the reduced density gradient and with a dependence on the kinetic energy density^[1,2] show an impressive performance for weak interactions that are crucial for the structure of biomolecules in both condensed phase and under isolated vacuum conditions.^[3–6] Even in conjunction with a well converged basis set, geometry optimizations for systems up to few hundred atoms are feasible. Unfortunately, for such a size a thorough screening of the complete conformational space is still not possible. More approximate techniques, such as classical force fields or semi empirical quantum mechanical (QM) methods have to be used for this purpose. Here, we test the performance of different methods, including classical nonpolarizable and polarizable force fields and a semiempirical DFT method, with respect to their ability of reproducing the relative energetics of a medium-sized biomolecule. As reference data, we use the results of a hybrid-meta GGA DFT method, which we have previously validated against experimental data^[7] and has been confirmed at a similar theoretical level by others.^[8,9]

[a] M. Doemer, M. Guglielmi, P. Athri, I. Tavernelli, U. Rothlisberger
Laboratoire de Chimie et Biochimie Computationnelle, Institut des Sciences
et Ingénierie Chimique, École Polytechnique Fédérale de Lausanne,
1015 Lausanne, Switzerland
E-mail: ursula.rothlisberger@epfl.ch

[b] N. S. Nagornova, T. R. Rizzo, O. V. Boyarkin,
Laboratoire de Chimie Physique Moléculaire, Institut des Sciences
et Ingénierie Chimique, École Polytechnique Fédérale de Lausanne,
1015 Lausanne, Switzerland

Contract grant sponsor: SNF; contract grant numbers: 200020-120065, 200020-130082, 200020-130579; contract grant sponsor: EPFL; contract grant sponsor: NCCR-MUST interdisciplinary research program.

© 2012 Wiley Periodicals, Inc.

As a test set, we use a pool of nine gas-phase conformations of protonated gramicidin S (GS), a cyclic decapeptide with the highly symmetric sequence cyclo-ValOrnLeuPheProValOrnLeuPhePro, where Orn designates ornithine and Phe is the D rather than the L enantiomer. GS is a natural antibiotic peptide against Gram-positive and -negative bacteria and several pathogenic fungi.^[10,11] The proposed mechanism of action is based upon distortions caused by its binding to the microbial cell membranes. Unfortunately, it appears to be toxic to human blood cells. GS has been studied extensively in the condensed phase,^[12–18] but no structure in its native membrane environment is available. A better understanding of its structure and interactions with the solvent and cell membranes might help in the rational design of GS analogs with reduced hemolytic activity and preserved antimicrobial features. In this respect, it is important to know the intrinsic structure of gramicidin S in the absence of any solvent and environment effects.

The experimental data (frequencies, intensities of vibrational transitions and their partial assignment), which we use as a reference for validation of our calculations, were obtained by measuring conformer-selective IR spectra of the protonated species $[GS + 2H]^{2+}$ isolated in the gas phase at $T \sim 12$ K. The isolation of the target biomolecules removes their interaction with the solvent, revealing weak intramolecular interactions that control structure and stability, while the cryogenic cooling suppresses different types of inhomogeneous spectral broadening and condenses most of the species at their vibrational ground levels. Conformational selectivity of these measurements greatly simplifies the comparison with calculated vibrational spectra, since the latter are obtained separately for each computed molecular structure. In addition to the frequencies and intensities of vibrational transitions, the experiment provides some structural information, such as the relative proximity of certain chemical groups or the relative number of hydrogen bonds. However, it is still a very challenging task to deduce a 3D molecular structure (Figure 1) from the vibrational spectrum (Figure 2) alone. Computational techniques can be applied to determine the optimal arrangement of the nuclei and to calculate the corresponding vibrational spectrum. Matching the calculated with the experimental IR spectrum can then be used to identify the equilibrium geometry.

Besides its pivotal role in identifying the intrinsic structure of biomolecules, cold ion spectroscopy, as described in more detail in the Methodology section, also provides valuable benchmark data for theoretical methods.^[19] The gas-phase environment renders the system feasible for first principles electronic structure methods and the highly resolved experimental IR spectra allow, in combination with isotope substitution experiments, direct assignments with respect to the calculated vibrational bands. Before attempting to solve the 3D structure of cold protonated Gramicidin S, we have performed benchmarking studies on bare and microsolvated protonated tryptophan in which we have assessed the performance of various popular DFT methods to predict the lowest energy structure in comparison with high level wave function based methods (CBS-C,^[20] see Supporting Information for a brief description) and experiments.^[21] It turned out, that in all cases CBS-C was able to predict the lowest energy

isomers that are in agreement with the experimentally observed vibrational spectra. M06² and M05-2X¹ provided energetics in close agreement with the CBS-C results, but only M05-2X and B3LYP^[22–25] yielded highly-reliable predictions of the vibrational spectra.

In this work we extend our benchmarking effort to a larger size biomolecule, i.e., gas-phase $[GS + 2H]^{2+}$. In particular, we tested the performance of the classical force fields AMBER FF96,^[26] FF99SB,^[27] FF02polEP^[28] and AMOEBA^{bio09}^[29] as well as the semiempirical self-consistent charge density functional tight-binding (SCC-DFTB) method^[30] in predicting the relative energetics of a pool of nine conformers with respect to the M05-2X/6-31G(d,p) level of theory. The latter has been confirmed as a suitable reference method that predicts the correct ground state structure also for $[GS + 2H]^{2+}$, as verified by comparison to experiment.^[7]

Methodology

Geometry optimizations at the classical level using the FF96, FF99SB, and FF02polEP force fields were performed via simulated annealing as implemented in the AMBER9 software.^[31] The time step was set to 1 fs, bonds involving Hydrogen atoms were constrained using the SHAKE algorithm.^[32] The temperature was controlled by a Langevin thermostat with a collision frequency of 3.0 ps^{-1} . Heating for 3 ns, equilibration for 5 ns and linear cooling for 20 ns. The SCC-DFTB method was used as implemented in DFTB+, v.1.1^[33] in conjunction with the mio-0-1 parameter set.^[30,34] Improvements for the description of hydrogen bonding^[35] and dispersion interactions^[36] were considered as well and will be denoted as SCC-DFTB(h) and SCC-DFTB(d), respectively. Geometry optimizations were performed up to a convergence of 10^{-4} a.u. of the atomic forces.

DFT calculations with the M05-2X functional were performed using Gaussian G09,^[37] using the 6-31G(d,p) basis set, tight convergence criteria and the UltraFine integration grid option.

The experimental procedure to detect the conformer-selective vibrational spectra involved a combination of electrospray ionization, mass spectrometry, cryogenic cooling, and laser spectroscopy. The protonated peptides in the gas phase were produced directly from an aqueous solution using a nano spray ion source. In a quadrupole mass filter the parent ions were pre-selected according to their mass-to-charge ratio and then transferred to a 22-pole ion trap, where they were cooled to ~ 6 K by collision with cold helium. At this temperature, vibrational resolution is possible even for a system as large as a decapeptide. Conformer-selective vibrational spectra were measured by using IR/UV double resonance detection, where vibrational pre-excitation of the biomolecular ions by an IR pulse alters their subsequent UV fragmentation yield.^[38–41] For more details see the Supporting Information of Ref. [7].

Results

We have selected nine structures of $[GS + 2H]^{2+}$, chosen from simulated annealing runs at the classical level or structural modifications from these, for our benchmarking study on the energetics of a range of methods. Table 1 labels the different conformation

Table 1. Characteristic structural parameters for conformations R01-R09 optimized at the M05-2X/6-31G(d,p) level of theory.

Name	No free backb. NHs	Struc. RMSD (Å)	NH ₃ -Phe	Phe-Phe
R01	0	0.00	2.95, 2.97	14.94
R02	0	0.70	2.95, 2.97	15.18
R03	0	0.74	2.96, 2.96	15.27
R04	2	2.68	8.74, 8.74	15.36
R05	4	2.07	6.52, 6.53	19.64
R06	4	2.35	6.27, 6.64	18.86
R07	3	3.16	3.19, 5.96	14.80
R08	2	1.94	5.02, 5.02	13.70
R09	6	5.53	2.96, 2.96	4.47

Hydrogen bond analysis (distance cutoff: 3.5 Å, angle cutoff: 70°). Total number of free backbone NHs, structural RMSD with respect to the minimum energy conformation (R01) and shortest distances between the ammonium and phenyl groups (Å).

according to their relative energy after geometry optimization at the M05-2X/6-31G(d,p) level of theory. R02, R07, R08, and R09 resulted from restrained simulated annealing runs using experimentally derived restraints, as described in the Supporting Information of Ref. [7]. In R02 one Orn side chain is bent inside with respect to the backbone ring, while the other is bent outside (O:in,out). R03 and R01 were derived from R02 to produce the (O:out,out) and (O:in,in) conformation, respectively (see Fig. 3). R04 resulted from simulated annealing runs at the classical level, using both the FF99SB and FF02 force field. R05 resulted from a geometry optimization starting with the coordinates of the crystal structure reconstructed from Ref. [18]. R06 resulted from multiple simulated annealing runs at the AMOEBA level.

Table 1 summarizes some key structural features of the selected conformations. Due to space limitations pictures are only reproduced for R01-R03 (Fig. 3), R06 (Fig. 4) and R09 (Fig. 5). Since R01-R03 differ by only slight variations in the Orn side chains the RMSDs are naturally very small. All backbone NHs are saturated with hydrogen bond interactions, the ammonia groups are in relative close proximity of the phenyl rings and the two phenyl rings are separated by ≈ 15 Å. The RMSD of R04 (2.7 Å) is relatively large and also visual inspection (see coordinates in Supporting Information) let us characterize this isomer as a qualitatively different structural type, where the main difference lies in the phenyl rings that are oriented in a parallel alignment with the proline rings instead of forming $\text{NH}_3^+ - \pi$ interactions. In this way, one of the hydrogens on each NH_3^+ group is not involved in any intramolecular interaction, while the other two are engaged in hydrogen bonds to the backbone. Judging from RMSD, number of free backbone NHs and distances between the NH_3^+ and Phe groups, structures R05 and R06 are very similar, but differ significantly from R01-R03. Structures R07-R09 feature RMSDs with respect to R01 ≥ 2 Å and from 2 to 6 free backbone NHs. Also, the NH_3 -Phe distances are higher in these structures than in R01-R03, except in R09. The latter features the highest number of free backbone NHs and RMSD value with respect to R01. The packing between the π systems of the two Phe side chains is optimized by placing them in a parallel arrangement above the ring of the backbone (see Fig. 5). Thereby the Phe-Phe

distance is reduced to only 4.5 Å. The NH_3^+ groups are oriented to form one hydrogen bond to the backbone (opposed to two in R01) and a $\text{NH}_3^+ - \pi$ interaction, whereas the third hydrogen atom is not involved in any intramolecular interaction.

Figure 1 shows the lowest energy conformation R01 color coded according to the RMSD with respect to the crystal structure derived from X-ray diffraction on the crystallized, hydrated species (Also see Figs. 3 and 4 for comparison).^[18] The highly symmetric structure of R01 is slightly more compact with an RMSD of the backbone atoms of ≈ 1 Å. Atoms with an RMSD of 2 Å or more are colored in dark red. The highest RMSDs (3–7.5 Å) are observed for the phenyl rings, which are oriented in a parallel way in order to optimize the $\text{NH}_3^+ - \pi$ interactions, in contrast to the crystal structure, where the NH_3^+ groups are partially solvated by crystal water. The RMSDs of the Orn side chain atoms are increasing for atoms closer to the ammonium groups (from ≈ 0.5 to 2 Å), reflecting the effect of the hydrogen bonds of the ammonium group to the backbone carbonyls, which are missing in the crystal structure. The highest RMSDs are found for the Leu side chains, as expected from these relatively flexible regions, (2–3 Å) and in the Pro side chains (≈ 2 Å), which seems to be due to a more compact folding of the backbone and the additional $\text{NH}_3^+ - \pi$ interactions in R01. This analysis illustrates the differences between the “intrinsic” lowest energy structure and the crystal structure, where packing effects and interaction with crystal water can cause significant deviations.

All geometries were optimized at the M05-2X/6-31G(d,p) level of theory and the first row in Table 2 gives the relative energetics for the pool of structures R01-R09. As expected from their structural similarity, R01-R03 are relatively close in energy, where each Orn bent outwards instead of inwards with respect to the backbone accounts for a destabilization of ~ 3.3 kcal/mol at the DFT level. Interestingly, the relative energy of R04 is of the same order as the one of R03, despite the differences in the structural features, as discussed above. Conformations R05 and R06 are relatively similar and their relative energy is almost the same. Conformations R07-R09 are energetically well separated from the others, with R09 being 43 kcal/mol higher in energy than

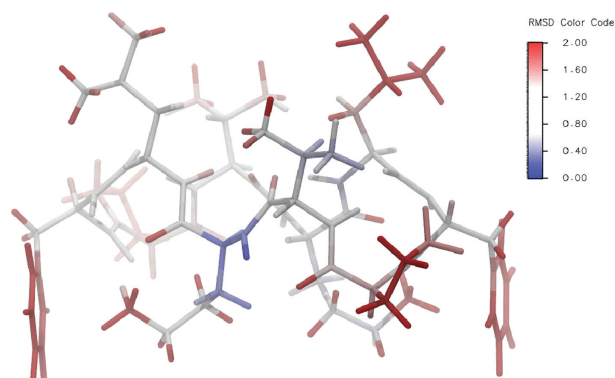


Figure 1. Conformation R01 optimized at the M05-2X/6-31G(d,p) level of theory. Color coding according to the RMSD with respect to the crystal structure reconstructed from Ref. [18]. [Color figure can be viewed in the online issue, which is available at wileyonlinelibrary.com.]

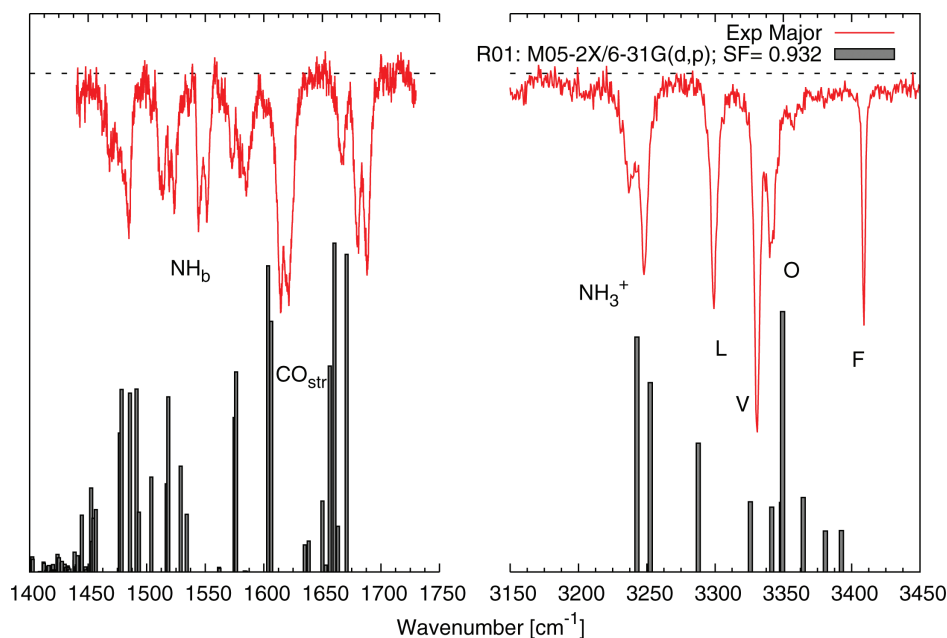


Figure 2. Calculated vibrational spectrum of R01 at the M05-2X/6-31G(d,p) level of theory (scaled by a constant factor of 0.932), compared to the experimental spectrum of the major isomer. [Color figure can be viewed in the online issue, which is available at wileyonlinelibrary.com.]

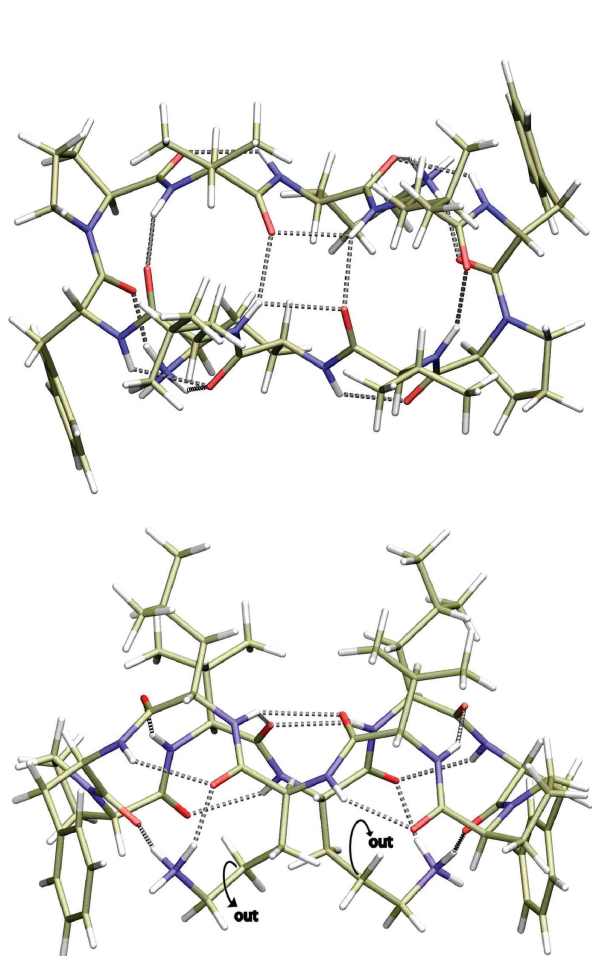


Figure 3. R01 top and side view. Arrows indicate structural changes that lead to conformations R02(Orn:in,out) and R03(Orn:out,out). [Color figure can be viewed in the online issue, which is available at wileyonlinelibrary.com.]

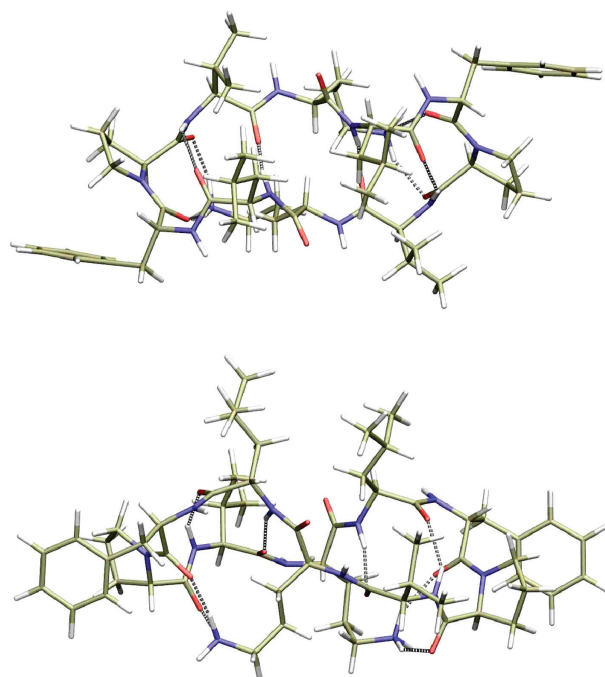


Figure 4. R06 top and side view. [Color figure can be viewed in the online issue, which is available at wileyonlinelibrary.com.]

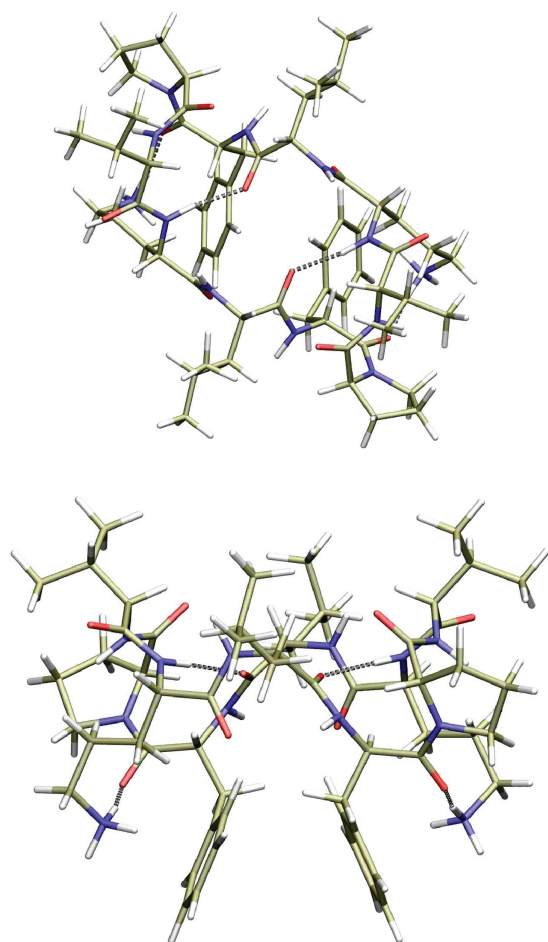
R01. The nine best structures of the pool thus span an approximate energy range from 4 kcal/mol to higher energy isomers at ~40 kcal/mol.

Experimentally gas-phase $[GS + 2H]^+$ at ~10 K is present in three different conformations, one of which is significantly more abundant than the other two.^[7,19] For the major isomer three characteristic features can be deduced from experimental data: (1) it is highly symmetric, (C_2); (2) the observed frequencies of the

Table 2. Relative energetics of nine $[GS + 2H]^{2+}$ conformations in kcal/mol with respect to the lowest energy structure at the M05-2X/6-31G(d,p) level.

Method	R01	R02	R03	R04	R05	R06	R07	R08	R09	RMSD	MAX
M05-2X	0.00	3.64	6.57	6.77	[~ 8.69]	8.70	16.42	22.19	43.33	–	–
DFTB	0.00	2.95	4.08	1.95	4.31	5.48	6.36	5.48	31.15	8.09	16.72
DFTB(h)	0.00	3.17	6.07	4.60	9.39	8.97	10.03	8.40	16.09	10.43	27.24
DFTB(d)	0.00	3.09	6.56	4.79	0.74	–0.30	2.77	11.27	28.43	8.67	14.90
DFTB(h,d)	0.00	2.90	6.29	5.41	4.63	1.05	3.03	12.05	30.44	7.64	13.39
AMOEBA	0.00	4.75	8.57	14.09	6.71	–3.72	17.30	32.25	43.16	5.95	12.42
FF02	0.00	–0.41	13.06	–18.35	12.24	–0.69	–8.72	0.32	9.69	18.36	33.64
FF99SB	0.00	1.87	2.13	–6.88	–2.20	–3.25	–1.83	10.26	22.63	12.36	20.70
FF96	0.00	1.50	1.33	4.30	–5.32	–6.17	3.12	19.68	29.49	9.60	14.87

The lowest energy structure for each respective method is highlighted in bold. The energy of R05 at the M05-2X level has to be considered as approximate only. Due to the intrinsic difficulties of the structure, convergence could only be reached up to within 0.01 kcal/mol.

**Figure 5.** R09 top and side view. [Color figure can be viewed in the online issue, which is available at wileyonlinelibrary.com.]

Val and Leu NH stretch vibrations can only originate from structures in which the backbone NH of these residues are hydrogen bonded; and (3) the ammonium groups of the Orn residues are in close proximity to the aromatic rings of the phenylalanines. All of these features are reproduced by the lowest energy conformation at the M05-2X level (R01) as discussed above and in Table 1. A stringent test for the identification of the lowest energy structure was the comparison of the calculated and experimental

vibrational spectrum, as reproduced in Figure 2. The theoretical predictions are in very good agreement with the experimental signals, in particular all experimentally assigned bands are correctly reproduced (see Ref. [7] for a detailed discussion).

The variety in the structural features among the pool of conformations R01–R09 render it an ideal selection for the benchmarking of different methods. The challenge is to reproduce the small energy separations between very similar structures, such as R01–R03 or R05–R06, and at the same time to account for structures that differ by up to 43 kcal/mol in energy. Table 2 compares the performance of various more approximate methods in reproducing the energetics at the M05-2X/6-31G(d,p) level of theory. Standard SCC-DFTB is able to predict the correct lowest energy conformer with respect to M05-2X. The largest errors occur in the high-energy conformations R07–R09, with a maximum error of 16.72 kcal/mol and an RMSD of the energies of all conformers of 8.1 kcal/mol. The hydrogen bonding corrected version DFTB(h) improves the energetics, but not enough for the high energy conformations, resulting in a maximum deviation of 27.2 kcal/mol for R09 and an RMSD of 10.4 kcal/mol. The dispersion corrected DFTB is the only variant, that is not able to identify the correct lowest energy conformation, but the three conformations R01, R05, and R06 appear as almost energetically degenerate. The best variant, in terms of RMSD (7.6 kcal/mol) and maximum deviation (13.4 kcal/mol) appears to be the combination DFTB(h,d). Note however, that the standard parameter set (mio-0-1) for the N–H interactions produces rather large errors in the proton affinities on sp^3 hybridized nitrogen species.^[42] This resulted in chemically unrealistic protonation states in molecular dynamics simulation of $[GS + 2H]^{2+}$ at finite temperature. It was therefore not possible to use the SCC-DFTB method for an extended sampling of the conformational space of $[GS + 2H]^{2+}$ as in a simulated annealing protocol, for example. The polarizable force field AMOEBA performs best, among the methods tested here, in terms of RMSD (6.0 kcal/mol) and maximum deviation (12.4 kcal/mol), but it predicts R01, the lowest energy structure at the DFT level, at 3.7 kcal/mol higher than R06. When compared to the other tested methods the overall energetic ordering is reproduced best, although not in all cases and for some the energy differences are overestimated. Both Amber force fields FF02polEP and FF99SB predict R04 as the lowest energy conformation, where the average error is very large (12 kcal/mol for

both methods), compared to the overall energy range tested. FF99SB performs slightly better in terms of RMSD and maximum deviation (12.4 and 20.7 kcal/mol) than FF02polEP, which shows the largest errors in both RMSD (18.4 kcal/mol) and maximum deviation (33.6 kcal/mol) among the selected methods. FF96 performs best among the Amber force fields tested here, with an RMSD and maximum deviation (9.60 kcal/mol and 14.87 kcal/mol) in the range of the DFTB variants. In contrast, FF96 predicts, like AMOEBA and DFTB(d), R06 as the lowest energy conformation (6.2 kcal/mol below R01).

Discussion and Conclusions

We have presented a pool of conformations for gas-phase protonated gramicidin S that covers a wide range of structural features and energy separations. This poses stringent constraints on the accuracy of the used computational methods. The lowest energy conformation at the M05-2X level of theory has been validated with experimental data, measured by cold ion spectroscopy. This experimental technique can produce highly resolved experimental benchmark data on biologically and biochemically relevant systems to test the performance of state of the art computational methods. From the work presented here and other benchmarking efforts on protonated tryptophan,^[21] we propose the family of Minnesota functionals as reliable reference methods for the energetics and especially M05-2X for the calculation of vibrational frequencies.

We have tested several more approximate methods including SCC-DFTB and its variants, as well as AMOEBA and AMBER FF02polEP, FF99SB, and FF96 for their performance in reproducing the energetics at the M05-2X level of theory of our pool of conformations. SCC-DFTB is the only method among the ones tested in this work, that predicts the correct lowest energy structure. Unfortunately, at the current state of the standard parameter set suggested for bio-molecular systems, the N–H interactions are not represented in a balanced manner, biasing sampling of unphysical protonation states. Without further methodological improvements on this side, it is therefore to be excluded as an initial sampling tool. AMOEBA, in contrast, shows slightly better energetic ordering, better RMSD values and maximum deviations, in particular for the high energy structures.

Unrestrained simulated annealing runs at the classical level did not lead to structures in agreement with the experimental observations (1)–(3). The two AMBER force fields, FF99SB and FF02polEP, and AMOEBA suggest conformations that are between 7 and 9 kcal/mol higher in energy than the minimum at the M05-2X level and show significantly different structural features. Surprisingly, simulated annealing using the FF02polEP force field results in the same conformation as FF99SB. Although both force fields were tailored to condensed phase properties of biological molecules the polarization could be expected to help transferability to the gas-phase environment. Even more surprising is, that the energetic ranking on the selected conformations is worse with the FF02polEP than with the FF99SB and FF96 force fields. The latter is the best Amber force field tested in this work, but nevertheless it favors conformations with significantly higher relative energies at the M05-2X level. We therefore

conclude that all three force fields can not be used reliably for the energetic prescreening of candidate structures and sample mostly unrealistic regions of the potential energy surface.


Among the protocols tested in this work, only the incorporation of structural restraints derived from experimental information in the conformational search at the FF99SB level lead to candidate structures with the desired structural features for the experimentally observed major conformation. The approximate methods tested here, seem not to be suitable for a reliable unbiased prescreening of candidate structures in the absence of experimental structural informations. Although AMOEBA and SCC-DFTB perform significantly better than the AMBER force fields, their RMSD and maximum deviations are still high compared to the overall energy differences between the individual conformations calculated at the M05-2X level.

Acknowledgments

The authors thank the CSCS and the CADMOS project for the computer time.

Keywords: density functional theory • density functional tight-binding • force field • peptides • cold ion spectroscopy

How to cite this article: M. Doemer, M. Guglielmi, P. Athri, N. S. Nagornova, T. R. Rizzo, O. V. Boyarkin, I. Tavernelli, U. Rothlisberger, *Int. J. Quantum Chem.* **2013**, *113*, 808–814. DOI: 10.1002/qua.24085

 Additional Supporting Information may be found in the online version of this article.

- [1] Y. Zhao, N. E. Schultz, D. G. Truhlar, *J. Chem. Theory Comp.* **2006**, *2*, 364.
- [2] Y. Zhao, D. G. Truhlar, *Theor. Chem. Acc.* **2008**, *120*, 215.
- [3] E. G. Hohenstein, S. T. Chill, C. D. Sherrill, *J. Chem. Theory Comp.* **2008**, *4*, 1996.
- [4] J. Jiang, Y. Wu, Z.-X. Wang, C. Wu, *J. Chem. Theory Comp.* **2010**, *6*, 1199.
- [5] Y. Zhao, D. G. Truhlar, *Chem. Phys. Lett.* **2011**, *502*, 1.
- [6] J. Cao, T. van Mourik, *Chem. Phys. Lett.* **2010**, *485*, 40.
- [7] N. S. Nagornova, M. Guglielmi, M. Doemer, I. Tavernelli, U. Rothlisberger, T. R. Rizzo, O. V. Boyarkin, *Angew. Chem. Int. Ed.* **2011**, *50*, 5383.
- [8] P. Kupser, K. Pagel, J. Oomens, N. Polfer, B. Koks, G. Meijer, G. von Helden, *J. Am. Chem. Soc.* **2010**, *132*, 2085.
- [9] K. Joshi, D. Semrouni, G. Ohanessian, C. Clavaguera, *J. Phys. Chem. B* **2011**, *116*, 483.
- [10] L. H. Kondejewski, S. W. Farmer, D. S. Wishart, R. E. W. Hancock, R. S. Hodges, *Int. J. Pept. Prot. Res.* **1996**, *47*, 460.
- [11] L. H. Kondejewski, S. W. Farmer, D. S. Wishart, C. M. Kay, R. E. W. Hancock, R. S. Hodges, *J. Biol. Chem.* **1996**, *271*, 25261.
- [12] D. T. Warner, *Nature* **1961**, *190*, 120.
- [13] S. E. Hull, R. Karlsson, P. Main, M. M. Woolfson, E. J. Dodson, *Nature* **1978**, *275*, 206.
- [14] Y. Xu, I. P. Sugár, N. R. Krishna, *J. Biomol. NMR* **1995**, *5*, 37.
- [15] G. Tishchenko, V. Andrianov, B. Vainstein, M. Woolfson, E. Dodson, *Acta Crystallogr. D* **1997**, *53*, 151.
- [16] E. J. Prenner, R. N. A. H. Lewis, R. N. McElhaney, *Biochim. Biophys. Acta - Biomembrs.* **1999**, *1462*, 201.
- [17] E. Pittenauer, M. Zehl, O. Belgacem, E. Raptakis, R. Mistrik, G. Allmaier, *J. Mass Spectrom.* **2006**, *41*, 421.
- [18] A. L. Llamas-Saiz, G. M. Grotenbreg, M. Overhand, M. J. van Raaij, *Acta Crystallogr. D* **2007**, *63*, 401.

- [19] N. S. Nagornova, T. R. Rizzo, O. V. Boyarkin, *J. Am. Chem. Soc.* **2010**, *132*, 4040.
- [20] P. M. Mayer, C. J. Parkinson, D. M. Smith, L. Radom, *J. Chem. Phys.* **1998**, *108*, 604.
- [21] M. Guglielmi, M. Doemer, P. Athri, N. Nagornova, O. V. Boyarkin, T. R. Rizzo, I. Tavernelli, U. Rothlisberger, (In preparation).
- [22] A. D. Becke, *J. Chem. Phys.* **1993**, *98*, 5648.
- [23] C. Lee, W. Yang, R. Parr, *Phys. Rev. B* **1988**, *37*, 785.
- [24] S. Vosko, L. Wilk, M. Nursair, *Can. J. Phys.* **1980**, *58*, 1200.
- [25] P. J. Stephens, F. J. Devlin, C. F. Chabalowski, M. J. Frisch, *J. Phys. Chem* **1994**, *98*, 11623.
- [26] P. A. Kollman, R. Dixon, W. Cornell, T. Fox, C. Chipot, A. Pohorille, In *Computer Simulation of Biomolecular Systems: Theoretical and Experimental Applications*, edited by A. Wilkinson, P. Weiner, W. F. van Gunsteren (Kluwer/Escom, Dordrecht, 1997), Vol. 3, pp. 83–96.
- [27] V. Hornak, R. Abel, A. Okur, B. Strockbine, A. Roitberg, C. Simmerling, *Proteins* **2006**, *65*, 712.
- [28] Z.-X. Wang, W. Zhang, C. Wu, H. Lei, P. Cieplak, Y. Duan, *J. Comp. Chem.* **2006**, *27*, 781.
- [29] P. Ren, C. Wu, J. W. Ponder, *J. Chem. Theory Comp.* **2011**, *7*, 3143.
- [30] M. Elstner, D. Porezag, G. Jungnickel, J. Elsner, M. Haugk, T. Frauenheim, S. Suhai, G. Seifert, *Phys. Rev. B* **1998**, *58*, 7260.
- [31] D. A. Case, T. A. Darden, T. E. Cheatham, III, C. L. Simmerling, J. Wang, R. E. Duke, R. Luo, K. M. Merz, D. A. Pearlman, M. Crowley, R. C. Walker, W. Zhang, B. Wang, S. Hayik, A. Roitberg, G. Seabra, K. F. Wong, F. Paesani, X. Wu, S. Brozell, V. Tsui, H. Gohlke, L. Yang, C. Tan, J. Mongan, V. Hornak, G. Cui, P. Beroza, D. H. Mathews, C. Schafmeister, W. S. Ross, P. A. Kollman, *AMBER* 9, 2006.
- [32] J.-P. Ryckaert, G. Ciccotti, H. J. C. Berendsen, *J. Comp. Phys.* **1977**, *23*, 327.
- [33] B. Aradi, B. Hourahine, T. Frauenheim, *J. Phys. Chem. A* **2007**, *111*, 5678.
- [34] General purpose parameter set for bio-organic systems available from <http://www.dftb.org/parameters> (1998).
- [35] H. Hu, Z. Lu, M. Elstner, J. Hermans, W. Yang, *J. Phys. Chem. A* **2007**, *111*, 5685.
- [36] L. Zhechkov, T. Heine, S. Patchkovskii, G. Seifert, H. A. Duarte, *J. Chem. Theory Comp.* **2005**, *1*, 841.
- [37] M. J. Frisch, G. W. Trucks, H. B. Schlegel, G. E. Scuseria, M. A. Robb, J. R. Cheeseman, G. Scalmani, V. Barone, B. Mennucci, G. A. Petersson, H. Nakatsuji, M. Caricato, X. Li, H. P. Hratchian, A. F. Izmaylov, J. Bloino, G. Zheng, J. L. Sonnenberg, M. Hada, M. Ehara, K. Toyota, R. Fukuda, J. Hasegawa, M. Ishida, T. Nakajima, Y. Honda, O. Kitao, H. Nakai, T. Vreven, J. A. Montgomery, Jr., J. E. Peralta, F. Ogliaro, M. Bearpark, J. J. Heyd, E. Brothers, K. N. Kudin, V. N. Staroverov, R. Kobayashi, J. Normand, K. Raghavachari, A. Rendell, J. C. Burant, S. S. Iyengar, J. Tomasi, M. Cossi, N. Rega, J. M. Millam, M. Klene, J. E. Knox, J. B. Cross, V. Bakken, C. Adamo, J. Jaramillo, R. Gomperts, R. E. Stratmann, O. Yazyev, A. J. Austin, R. Cammi, C. Pomelli, J. W. Ochterski, R. L. Martin, K. Morokuma, V. G. Zakrzewski, G. A. Voth, P. Salvador, J. J. Dannenberg, S. Dapprich, A. D. Daniels, Ö. Farkas, J. B. Foresman, J. V. Ortiz, J. Cioslowski, D. J. Fox, Gaussian 09, Rev. B.01; Gaussian, Inc., Wallingford CT, **2010**.
- [38] J. Carney, T. Zwier, *J. Phys. Chem. A* **2000**, *104*, 8677.
- [39] L. Snoek, E. Robertson, R. Kroemer, J. Simons, *Chem. Phys. Lett.* **2000**, *321*, 49.
- [40] R. Page, Y. Shen, Y. Lee, *J. Chem. Phys.* **1988**, *88*, 5362.
- [41] C. J. Gruenloh, J. R. Carney, F. C. Hagemeister, C. A. Arrington, T. S. Zwier, *J. Chem. Phys.* **1998**, *109*, 6601.
- [42] Y. Yang, H. Yu, D. York, Q. Cui, M. Elstner, *J. Phys. Chem. A* **2007**, *111*, 10861.

Received: 12 January 2012

Revised: 12 January 2012

Accepted: 2 February 2012

Published online on 5 April 2012